Atmos. Chem. Phys. Discuss., 8, 17661–17690, 2008
www.atmos-chem-phys-discuss.net/8/17661/2008/

Atmospheric Chemistry and Physics Discussions

This discussion paper is/has been under review for the journal *Atmospheric Chemistry and Physics (ACP)*. Please refer to the corresponding final paper in *ACP* if available.

MAX-DOAS measurements in southern China: 1. automated aerosol profile retrieval using oxygen dimers absorptions

X. Li[1,2], T. Brauers[2], M. Shao[1], R. M. Garland[3], T. Wagner[4], T. Deutschmann[5], and A. Wahner[2]

[1]College of Environmental Sciences and Engineering, Peking University, Beijing, China
[2]Institute for Chemistry and Dynamics of the Geosphere (ICG-2), Forschungszentrum Jülich, Germany
[3]Biogeochemistry Department, Max Planck Institute for Chemistry, Mainz, Germany
[4]Satellite Group, Max Planck Institute for Chemistry, Mainz, Germany
[5]Institute for Environmental Physics, Universität Heidelberg , Heidelberg, Germany

Received: 25 July 2008 – Accepted: 22 August 2008 – Published: 29 September 2008

Correspondence to: T. Brauers (th.brauers@fz-juelich.de)

Published by Copernicus Publications on behalf of the European Geosciences Union.

Abstract

We performed MAX-DOAS measurements during the PRiDe-PRD2006 campaign in the Pearl River Delta region 50 km north of Guangzhou, China, for 4 weeks in June 2006. We used an instrument which simultaneously sampled the wavelength range from 292 nm to 443 nm at 7 different elevation angles between 3° and 90°. Here we show that the O_4 (O_2 dimer) absorption at 360 nm can be used to retrieve the aerosol extinction and the height of the boundary layer. A comparison with simultaneously recorded, ground based nephelometer data shows an excellent agreement.

1 Introduction

Differential Optical Absorption Spectroscopy (DOAS) is a powerful technique for the measurement of trace gas concentrations in the atmosphere (Platt and Stutz, 2008). Multi-axis differential absorption spectroscopy (MAX-DOAS) is a relatively new technique which was developed recently (Hönninger et al., 2004) and was first used to retrieve bromine oxide profiles in the troposphere (Hönninger and Platt, 2002). The MAX-DOAS technique was successfully used by different groups to measure NO_2 (e.g. Leigh et al., 2007; Pikelnaya et al., 2007), HCHO (e.g. Inomata et al., 2008), glyoxal (e.g. Sinreich et al., 2007), and other uv or vis light absorbing molecules. Moreover, Wagner et al. (2004) developed a technique to use the O_4 absorption to retrieve aerosol profiles (Wittrock et al., 2004; Friess et al., 2006).

The general idea of MAX-DOAS is to record spectra of scattered sunlight at different elevation angles, α (the angle between the viewing direction of the telescope and the horizontal direction). The light path in the stratosphere is basically the same for all elevation angles. Therefore, the stratospheric contribution of trace gas absorption almost cancels out when a spectrum at an elevation angle $\alpha \neq 90^\circ$ is divided by a spectrum taken at $\alpha = 90^\circ$ at the same time and location.

For an individual measurement at elevation angle α, the measured optical density

ACPD

8, 17661–17690, 2008

refers to the slant column density (SCD) which is the concentration $C(s)$ of a species integrated along the paths s where the photons travelled

$$\mathrm{SCD}_\alpha = \int C(s)ds = \frac{1}{\sigma}\log\left(\frac{I_0}{I_\alpha}\right) \quad (1)$$

Here σ is the absorption cross section, I_0 is the reference spectrum, and I_α is the measured spectrum. Since the SCD strongly depends on the observation geometry and meteorological conditions, it is usually converted to vertical column density (VCD) which is the concentration integrated along the vertical path through the atmosphere.

$$\mathrm{VCD} = \int C(z)dz = \frac{\mathrm{SCD}_\alpha}{\mathrm{AMF}_\alpha} \quad (2)$$

The conversion from SCD to VCD is achieved by the air mass factor (AMF), i.e., the averaged light path enhancement for solar light traveling through the atmosphere compared to a straight vertical path (Perliski and Solomon, 1993).

For measurements focusing on the species in the troposphere, the idea of differential slant column density (DSCD) has been widely used (e.g. Irie et al., 2008; Pikelnaya et al., 2007). The DSCD is the difference of between the SCDs between $\alpha \neq 90^\circ$ and $\alpha = 90^\circ$.

$$\mathrm{DSCD}_\alpha = \mathrm{SCD}_\alpha - \mathrm{SCD}_{90^\circ} = \frac{1}{\sigma}\log\left(\frac{I_{90^\circ}}{I_\alpha}\right) \quad (3)$$

During the analysis of MAX-DOAS measurement, the DSCD can be directly retrieved by using the spectrum taken at $\alpha = 90^\circ$ of each measurement cycle as reference spectrum in the DOAS fit. For both, I_{90° and I_α, the light path in the stratosphere is nearly identical. Thus, the contribution of trace gas absorption in the stratosphere nearly vanishes.

In order to convert the DSCD_α into a tropospheric trace gas column a differential air mass factor DAMF_α needs to be calculated

$$\mathrm{DAMF}_\alpha = \mathrm{AMF}_\alpha - \mathrm{AMF}_{90^\circ} \quad (4)$$

ACPD
8, 17661–17690, 2008

from the difference of the respective air mass factors. The trace gas column in the troposphere, i.e.

$$\mathrm{VCD_{trop}} = \frac{\mathrm{DSCD}_\alpha}{\mathrm{DAMF}_\alpha} = \frac{\mathrm{SCD}_\alpha - \mathrm{SCD}_{90^\circ}}{\mathrm{AMF}_\alpha - \mathrm{AMF}_{90^\circ}} \quad (5)$$

is calculated from the slant column densities and air mass factors.

MAX-DOAS instruments can be very simple and easy to operate. They require a (small) telescope that can be directed to several directions in the sky, including the zenith. The second component is a spectrograph with a typical DOAS resolution of 0.1 nm to 1 nm. However, despite the simplicity of the experimental setup, the evaluation of MAX-DOAS measurements from measured spectra to aerosol and trace gas concentrations or profiles is a demanding task. This evaluation requires the use of radiative transfer modelling especially in situations where aerosol loads are high and multiple scattering occurs.

The radiative transfer models (RTMs) calculate the photon flux at a certain location (longitude, latitude, altitude) in the atmosphere depending on viewing direction, the solar position (zenith and azimuth angle) and a number of parameters describing absorption and scattering of photons on their way through the atmosphere. In polluted areas, the major influence on the photon paths besides clouds is the distribution of aerosol in the troposphere. In this study we concentrate on the effect of aerosols and investigate only measurements under mostly cloud free conditions. Over the last years, different radiative transfer models have been developed. In this study, we used McArtim (Deutschmann, 2008[1]) which is a backward Monte-Carlo model. In this model, a photon emerges from a detector in an arbitrary line of sight direction and is followed in the backward direction along the path until the photon leaves the top of the atmosphere or is absorbed. The various events which may happen to the photon at various altitudes are defined by suitable probability distributions. Random numbers decide on

[1]Deutschmann, T.: Atmospheric Radiative Transfer Modelling with Monte Carlo Methods, Univ. Heidelberg, Germany, diploma thesis to be submitted, 2008

the occurrence of events. At each scatter event a weight is calculated from the product of two terms. The first factor is the probability that the sunlight reaches the scatter event, the second is the phase function of the scatter event evaluated at the angle between the Sun direction and the direction of the sampled trajectory from the scatter event to the detector. For each trajectory an estimate of the sun normalized radiance is obtained by adding the weights of all scatter orders. A large number of random photon paths are generated, thus reproducing the light contributing to the simulated measurement.

RTMs were reviewed by Hendrick et al. (2006) and Wagner et al. (2007). Different RTMs differ in the way of simulating photon transverse process in the atmosphere, the treatment of the Earth's sphericity, the way of considering aerosol scattering, the inclusion of the photo-enhancement of short lifetime species, etc. Intercomparison activities demonstrate an agreement within 10% of simulated SCD and AMF of species like NO_2 and HCHO (Hendrick et al., 2006; Wagner et al., 2007). McArtim was compared intensively to Tracy-II, one of the participants in the comparison by Wagner et al. (2007) and was found to agree excellently[1]. The advantage of McArtim over Tracy-II is the improved computational speed and the increased number of output parameters.

The concept of aerosol retrieval from the oxygen dimer absorption was introduced by Wagner et al. (2004). The O_4 concentration is proportional to the square of O_2 concentration, and it mainly dependent on the temperature and pressure profile. Most of the O_4 resides in the lower part of the troposphere, therefore the O_4 DSCD is sensitive to changes in the photon paths, mainly at low altitudes. Aerosol particles lead to a variation of photon paths and thus a variation in the O_4 DSCDs. Therefore, the O_4 DSCD can be used as an indicator of the aerosol load in the atmosphere. In the condition of low aerosol load or the existence of clouds, the probability of multiple scattering increases, which will lead to the simultaneous increase of the O_4 DSCDs at all elevation angles. Under conditions of high aerosol load, the distance from which photons can reach the telescope will strongly decrease due to the high aerosol extinction. This will cause a strong reduction of O_4 DSCDs especially those measured at low elevation

angles. Meanwhile, the difference of O_4 DSCDs between low elevation angles will become quite small. The high aerosol extinction also shortens the penetration depth of the incident sunlight, which can be reflected by the decrease of the amplitude of O_4 DSCDs diurnal variation. Furthermore, since the aerosol scattering strongly prefers the forward direction, the O_4 DSCDs measured at azimuth towards the sun should be lower than those measured at azimuth. The magnitude of this difference depends on the frequency of aerosol scattering and on the scattering phase function.Wagner et al. (2004) explored the sensitivity on the parameters.

In this paper we use the oxygen dimer absorption at 360 nm to explore the aerosol profile at a semi-urban location in southern China. We have developed an automated method to retrieve the profile from the measured O_4 DSCDs. In forthcoming papers we will explore the trace gas absorptions.

2 Experimental

2.1 The MAX-DOAS instrument

The instrument is a Mini-MAX-DOAS (Fa. Hoffmann, Rauenberg, Germany). It containes a miniature crossed Czerny-Tuner spectrometer unit USB2000 (Ocean Optics Inc.) with a spectral resolution of ≈0.7 nm full width at half maximum (FWHM). The spectral range of 292 nm to 443 nm is mapped onto a one-dimensional CCD-detector with 2048 pixels. The spectrometer unit was cooled to a stable temperature of +19°C in order to minimize changes in optical properties of the spectrometer and to reduce detector dark current. The scattered sunlight was collected and focused by a quartz lens and was led into the spectrometer unit by a quartz fibre bundle. A stepper motor enabled the adjustment of the viewing direction to a desired elevation angle (i.e. the angle between the horizon and the pointing direction of the telescope). All functions were controlled by a laptop via USB connection.

The instrument was operated by a fully automated measurement program (MiniMax,

ACPD
8, 17661–17690, 2008

Udo Friess, University of Heidelberg). The program employed routines to adapt the integration time of the measurements to the light conditions in order to achieve a constant signal level (i.e. 80 % of the saturation of the CCD-detector), to store the spectra and to control the movements of the telescope. The instrument slit function was determined by measuring the emission line of a mercury lamp at 334 nm. Scattered sunlight spectra were acquired sequentially at elevation angles of 90° (i.e. zenith), 30°, 20°, 15°, 10°, 5° and 3°, representing one measurement cycle, taking 10 min to 15 min. The dark current and offset spectra were recorded every night.

2.2 The DOAS analysis

The O_4 DSCDs were determined by DOAS fit in the wavelength range between 351 nm and 389 nm. The logarithm of a Fraunhofer reference spectrum (FRS), several trace gas absorption cross sections, a Ring spectrum (Grainger and Ring, 1962), a third order polynomial and a second order offset polynomial were fit together to the logarithm of the measured spectrum already corrected for dark current and offset. During the fit, the measurement spectrum was allowed to shift and squeeze with respect to the FRS, the Ring spectrum and the absorption cross sections. The fitting procedure was conducted using the script mode of the DOASIS software (Kraus and Geyer, 2001).

Figure 1 illustrates one example of the DOAS fit recorded on 19 July 2006 at 10:59 at a solar zenith angle of 23° and an elevation angle of 3°. For each measurement cycle, the corresponding zenith spectrum (α=90°) was taken as FRS for the spectra at off-axis elevation angles. This largely eliminates the stratospheric contributions to the DSCDs. However, the O_4 DSCD is only marginally affected by stratospheric absorptions since O_4 mainly resides in the troposphere. The Ring spectrum was calculated from each measured spectrum (Bussemer, 1993). For the fit of the absorbing trace gases, we used high resolution absorption cross sections which were convolved by the instrument slit function to match the resolution of the instrument (except for O_4 spectrum which was interpolated). These references include HCHO (Meller and Moortgat, 2000), BrO (Wilmouth et al., 1999), NO_2 (Voigt et al., 2002), O_3 at 280 K (Voigt et al., 2001), and

ACPD
8, 17661–17690, 2008

O_4 (Greenblatt et al., 1990) with a manual adjustments of wavelength axis (R. Sinreich, personal communication).

In addition, the solar I_0-effect (Platt et al., 1997) was corrected for NO_2 and O_3 reference spectra with slant column density of 1.5×10^{17} cm^{-2} and 1.5×10^{20} cm^{-2}, respectively. The wavelength calibration was performed by fitting the Fraunhofer reference spectra to a high resolution Fraunhofer spectrum (Kurucz et al., 1984), convoluted with the instrument's slit function.

2.3 Setup of the instruments at the Guangzhou Backgarden supersite

Our MAX-DOAS observations were performed in the framework of the "Program of Regional Integrated Experiments of Air Quality over the Pearl River Delta" (PRIDE-PRD2006) (Zhang et al., 2008[2]), The intensive campaign took place from 3 July to 31 July in Pearl River delta area in southern China. Our measurements were conducted in Back Garden (BG) supersite (23.50° N, 113.03° E). Our "Mini-MAX-DOAS" device was installed on the top of a 10 m high hotel building, pointing to the east. The MAX-DOAS measurements were accompanied by a comprehensive suite of atmospheric measurements (Zhang et al., 2008[2]). In this study we used the nephelometer and photoacoustic spectrometer the aerosol scattering and absorption, which are described in a separate paper (Garland et al., 2008) and therefore only a brief description follows.

The total aerosol particle scattering coefficients and hemispheric backscattering coefficients at three different wavelengths (λ=450 nm, 550 nm, and 700 nm) were measured with an integrating nephelometer (Model 3563, TSI). The aerosol particle absorption coefficient at 532 nm was determined with a photoacoustic spectrometer (PAS; Desert Research Institute), which provides highly sensitive absorption measurements

[2]Zhang, Y. H., Hu, M., Liu, S. C., Wahner, A., Wiedensohler, A., Andreae, M. O., Kondo, Y., Kim, Y. J., Shao, M., Zhong, L. J., and Fan, S. J.: Continuous efforts to investigate regional air pollution in the Pearl River Delta, China: PRiDe PRD2006 campaign, Atmos. Chem. Phys., in preparation, 2008.

without interference by scattering signals (Arnott et al., 1999). The optical data were averaged for two minutes. The main aerosol inlet used for both instruments in this study was equipped with a PM10 inlet and a diffusion dryer with silica gel/molecular sieve cartridges (average sampling relative humidity 33%).

3 Radiative transfer modelling

The modelling of the O_4 DSCDs was performed by a backward Monte-Carlo approach with the treatment of multiple scattering in a fully spherical geometry, i.e. McArtim (Deutschmann, 2008[1]). This model requires a number of input parameters like altitude, solar zenith and azimuth angles, pressure, temperature, absorbing trace gases and aerosol optical parameters for each layer in the atmosphere. The layers can be prescribed by the users. In our model runs we calculated the O_4 altitude profile from the square of the O_2 profile of the US standard atmosphere. We also used the temperature, pressure, and trace gas profiles from the US standard atmosphere. However, these parameters are of minor importance for the O_4 columns under evaluation here. The major influence comes from the aerosol optical parameters and the aerosol altitude profile.

For the aerosol optical properties, we selected a constant single scattering albedo (SSA) and a constant asymmetry parameter (g, under the Henyey-Greenstein approximation) of 0.85 and 0.68, respectively. These were deduced from the nephelometer measurements and they refer to the average in the time frame between 06:00 and 19:00 (local time) for all days. We also set the surface albedo constant to 7%, a value also used by Irie et al. (2008). The sensitivity on the albedo is small: doubling the albedo change the modelled O_4 DSCDs by less than 5%. The sensitivities on the single scattering albedo and the asymmetry parameter are larger: 10% changes in SSA and g modify the modelled O_4 DSCDs by 10% and 17%, respectively.

For the aerosol profile, we setup two layers, i.e. the atmospheric boundary layer and the free troposphere, which can be described with a limited set of parameters. Since our measurements were conducted at six independent values of the elevation angle

only it is required that the profiles are parameterized with less than six parameters. Over source regions, it is assumed that the well mixed boundary layer fills with particles emitted or photochemically formed, while in the layer aloft the aerosol content quickly decreases with height. Observations in Asia (e.g. Sasano, 1996; Chiang et al., 2007) obtained these kinds of profiles.

Thus the extinction profile $E(z)$ was setup as two layers in the range from 0 km to 15 km

$$E(z) = \begin{cases} \tau \cdot F/H & z \le H \\ \beta \cdot \exp(-z/\xi) & z > H \end{cases} \quad (6)$$

where z is the height above ground. τ is the aerosol optical depth from ground to 15 km (i.e. in the entire troposphere) and F is the fraction of the total extinction τ in boundary layer. H is the height of the boundary layer, ξ is the scaling height for the aerosol in the free troposphere, and β is the norm for exponential factor. In order for τ being the integrated optical depth, $E(z)$ must obey the boundary condition

$$\int_{0\,\mathrm{km}}^{15\,\mathrm{km}} E(z)dz = \tau \quad (7)$$

which leads to a conditional equation for β.

$$\beta = \frac{(1-F)\cdot\tau}{\xi \cdot (e^{-H/\xi} - e^{-15\mathrm{km}/\xi})} \quad (8)$$

We also introduce the extinction at ground level $E_0 = \tau \cdot F/H$ that can be compared to local, ground based measurements.

With this input, the McArtim program calculates the set of O_4 DSCD for the six elevation angles R_α within 15 min on a typical state-of-the-art PC when 200 000 photon paths are calculated. In order to estimate the input parameters of McArtim (τ, F, ξ, and H) the weighted difference between model data R_α and the measured data M_α

$$\chi^2(\tau, F, \xi, H) = \sum_{\alpha=3^\circ}^{30^\circ} \left(\frac{M_\alpha - R_\alpha(\tau, F, \xi, H)}{\sigma(M_\alpha)} \right)^2 \quad (9)$$

ACPD
8, 17661–17690, 2008

must be iteratively minimized, requiring several hours to days for a single data point. We therefore created look-up tables (LUTs) that then are used as input for the fitting procedure.

We created two LUTs both using the same set of solar zenith angles, SZA, and relative azimuth angles, SRAA (see Table 1). These were not selected independently, since during the 4 week period they cover only a small band in the area of the possible values (Fig. 2). We also used the same single scattering albedo (SSA), asymmetry parameter (g), and surface albedo, as denoted above.

The main difference between the two LUTs are the number of free parameters for the aerosol profiles (Eq. 6). In case A4 we choose two free parameters (τ and F) and fixed H and ξ to the values given in Table 1. In contrast, in case A5 we varied all four parameters within the range given in Table 1. The motivation for A4 was to create a very simple profile. It consists of a layer at the ground which is well mixed throughout the day and a second layer with a fixed scaling height. The other set, A5, reflects the idea of a well mixed boundary layer with height variations over the course of the day.

The aerosol parameters were chosen to cover a wide range of possible situations in the LUTs for subsequent fitting. The number of required McArtim runs were 10 648 and 46 800, for cases A4 and A5, respectively, corresponding to approximately 100 days and 500 days of computer time. However, this could be distributed to ≈30 PCs during off-time hours.

The LUTs provide O_4 DSCDs, L_α, as a function of the elevation angle α (3°, 5°, 10°, 15°, 20°, and 30°) and of the parameters τ and F for A4, and τ, F, ξ, and H for A5, respectively. For one measured cycle of O_4 DSCDs, M_α, we fitted the linearly interpolated values $L_\alpha(\tau, F, \xi, H)$ of the LUT (as a approximation for the $R_\alpha(\tau, F, \xi, H)$ in Eq. 9). In order to reduce the atmospheric variations as well as measurement noise of a single observation, the profile retrieval was applied for measured O_4 DSCDs averaged over one hour. The minimization procedure was conducted automatically using mpfit (Markwardt, 2008[3]) an implementation of the Levenberg-Marquardt algorithm. The

[3]Markwardt, C. B.: mpfit – Robust non-linear least squares curve fitting, http://cow.physics.

ACPD
8, 17661–17690, 2008

errors of the retrieved parameters were derived from the fitting procedure.

4 Results and discussion

The MAX-DOAS instrument was operated for the entire campaign period from 3 July 2006 to 25 July 2006. However, since most days of the campaign were characterized by clouds, we selected 9 virtually cloud-free days for this study on aerosols (Fig. 3). In the figure we see the influence of the elevation angle, the diurnal variation of the O_4 DSCD with the solar zenith angle and the effect of the aerosols. Wagner et al. (2004) show that aerosol particles close to the surface would reduce the difference of O_4 DSCDs between the different elevation angles as well as the magnitude of the O_4 DSCDs, providing a qualitative way to identify high aerosol load conditions. For example, the strong decrease of O_4 DSCDs in the last 3 days reflects the increased of aerosol load, also observed by in-situ measurements.

Figure 4 demonstrates two examples of the aerosol profile retrieval. The left column (Fig. 4a,c) shows the result for 21 July 2006 in the time interval from 11:00–12:00. For the two-parameter A4 model, the best fit (Fig. 4a) is reached when τ and F are $(0.15\pm0.01)\,\mathrm{km}^{-1}$ and 0.32 ± 0.05, respectively. The respective profile (Fig. 4c) indicates the majority of the aerosol in the 400 m layer at the ground. Differently, the 4-parameter model A5 provides a higher extinction in a thicker layer. The retrieved parameters are $\tau=0.81\pm0.21\,\mathrm{km}^{-1}$, $F=0.40\pm0.08$, $H=0.63\pm0.08\,\mathrm{km}$, and $\xi=30\pm11\,\mathrm{km}$. Although the shapes of the two profiles are very similar, the overall amplitude (i.e. τ) differs a lot. The aerosol extinction at the ground derived from A5 ($E_0=0.51\pm0.18\,\mathrm{km}^{-1}$) is twice as large as that from A4 ($E_0=0.24\pm0.04\,\mathrm{km}^{-1}$).

Another case study is presented for 24 July 2006, 12:00–13:00 (right column, Fig. 4b,d). Here the best fit is reached for A4 at $\tau=1.40\pm0.06\,\mathrm{km}^{-1}$ and $F=0.13\pm0.01$ and for A5 at $\tau=1.7\pm4.0\,\mathrm{km}^{-1}$, $F=0.5\pm0.8$, $H=1.0\pm2.5\,\mathrm{km}$, and $\xi=9\pm93\,\mathrm{km}$ (Fig. 4b).

wisc.edu/~craigm/idl/fitting.html, 2008.

ACPD
8, 17661–17690, 2008

The error in the parameters of A5 are caused by the covariances of the fitted parameters and indicate the small sensitivity of the O_4 DSCDs to changes in parameters.

The difference of the agreement between the aerosol profiles retrieved by A4 and A5 indicates that the two kinds of profile definition have different sensitivities to the retrieval. In the profile definition of A4, the height of the lowest layer was fixed to 0.4 km. When the aerosol load is very high, photons registered by the MAX-DOAS instrument at low elevation angles have not travelled a long distance in the atmosphere, due to the additional aerosol scattering and absorption. Under this condition, the MAX-DOAS O_4 observations are only sensitive to the aerosols distributed in a short vertical scale (when the horizontal aerosol distribution is assumed to be homogeneous). Thus, the best fit of modelled O_4 DSCDs against measured O_4 DSCDs is mainly dominated by the aerosol distribution near the ground-based instrument; the contribution from aerosols in upper layers is of minor importance. From this point of view, we can expect a good agreement between the aerosol profiles, especially the aerosol extinction in the lowest layer. The results demonstrate the existence of high aerosol extinction in the layer near the ground. Under these conditions, a high aerosol load was also observed by the nephelometer (Fig. 5). The total aerosol scattering at the O_4 absorption is calculated by extrapolating a second order polynomial fit to the measured total aerosol scattering at three different wavelengths to 360 nm (Eck et al., 1999). In the condition of low aerosol load, the sensitivity of the MAX-DOAS observations to upper aerosol layers (layers above 0.4 km or above H) increases. Since the profile definitions in these layers are quite different in A4 and A5, the results from the retrieval could be different as well.

In our retrieval processes, the aerosols in the lowest layer (i.e. 0–400 m and 0–H, for A4 and A5 respectively) are assumed to be distributed homogeneously (see Eq. 6). Therefore, the retrieved aerosol extinction in this layer E_0 can be compared to the simultaneous in-situ, ground-based nephelometer measurements. The nephelometer detects the aerosol total scattering (T_S) which is the major part of the extinction of ambient aerosols in most cases. The comparison of E_0 against T_S will under the assumption of constant aerosol in the lowest layer help us to validate our retrieval.

ACPD
8, 17661–17690, 2008

Figure 5 illustrates the time series of the converted nephelometer reading T_S and E_0 as derived from the runs A4 and and A5. The absolute value as well as the diurnal variation of aerosol extinction are very similar. Large differences between T_S and E_0 occur during morning hours. These can be attributed to several reasons: firstly, the nephelometer records the scattered light from the aerosol only which is the larger part of the light loss in most cases. However, the simultaneous in-situ photoacoustic spectrometer measurements demonstrated that the aerosol absorption during morning hours was high during most of the days. Secondly, an underestimation of the SSA will cause an overestimation of aerosol extinction by MAX-DOAS O4 observations. The SSA been used for the RTM was a constant value of 0.85. However, the measured SSA during the period when the discrepancies existed was usually lower than 0.85. Our sensitivity tests showed that the decrease of SSA by 5 % will lead to the decrease of modelled O_4 DSCDs by ≈5%. In order to achieve the best fit between modelled and measured O_4 DSCDs, the retrieval procedure will increase the aerosol extinction to compensate for the higher value of SSA. Thirdly, the existence of fog in morning hours can also influence the comparison between E_0 and T_S. The aerosol sampled by the nephelometer were first dried to ≈35% relative humidity. Therefore, the nephelometer is insensitive to changes in ambient relative humidity and the resulting impacts on the aerosol scattering. This is certainly not the case for MAX-DOAS observations. Meanwhile, the asymmetry parameter (g) and SSA of fog particles can be different from the values selected for the RTM calculation. Other causes for differences between MAX-DOAS and nephelometer could be small clouds or horizontal inhomogeneities cased by local emissions.

Given the arguments discussed above the correlation of E_0 and T_S is good. Based on the full dataset (N=90) the correlation coefficient is 0.87 (Fig. 6a). If we restrict the data to daytime hour between 11:00 and 19:00 (local time) the correlation coefficient is still 0.86 at N=54. A regression line drawn in the latter case yields a slope of 0.87 and an intercept 0.18 km^{-1}. Considering the fact that the MAX-DOAS measures the aerosol extinction averaged over a long distance while the nephelometer detects the

ACPD
8, 17661–17690, 2008

aerosol scattering in the air mass near the instrument, the results of the linear regression demonstrate a good agreement of the measurement results between these two instruments. As described above, the major discrepancies between E_0 and T_S were found during morning hours.

Using the 4 parameter model A5 we could retrieve aerosol profiles in the range from 0 to 15 km for all days plotted in Fig. 5. As an example, Fig. 7 shows the aerosol profiles of the different time intervals on 24 July 2006. The variation of aerosol vertical distribution can be clearly identified: In the early morning hours (06:00–08:00), aerosols from fog and local emission processes were concentrated in a surface layer of approximately 800 m. With the sun rising and growing convection the height of the lowest layer, H, increased and aerosols in this layer dispersed to upper layers. Due to this mixing process, the aerosol extinction in the lowest layer started to decrease. The highest value of H accompanied the lowest value of the extinction in the afternoon (16:00–17:00). The decrease of H and the accumulation of aerosols in the lowest layer starts again around sunset (18:00–19:00).

The diurnal cycle of H and E_0 on 24 July 2006 can be seen more clearly from Fig. 8. However, the values in the afternoon are highly variable when looking at one day only. Therefore, we accumulated all 9 days into one average diurnal profile (Fig. 9). The average mixing height was 0.8 km in early morning hours. It increased in the morning and reached the highest value of 1.9 km in the afternoon. Unfortunately, the boundary layer was not independently measured. The diurnal average aerosol extinction matches the nephelometer data in the afternoon. The differences in the morning clearly show the previously discussed underestimation of the nephelometer at high humidities.

5 Conclusions

In this study, the first MAX-DOAS measurements were performed in southern China. During a period of one month we encountered 9 days with no or marginal cloud cover. Under these conditions, we retrieved aerosol profiles from the absorption features of

the oxygen dimer, O_4, in the UV at 360 nm. The retrieval was based on multi-parameter lookup-tables, which were created by the radiative transfer model McArtim. We minimized the difference between the measured and modelled O_4 differential slant column as a function of the viewing geometry, i.e. the elevation angle of the MAX-DOAS telescope.

Two lookup-tables with different parametrization of the surface layer were created. One case assumed a surface layer with a fixed height of 400 m and only 2 free parameters (the total aerosol extinction τ and the fraction of aerosol in the surface layer F). The other LUT had 2 additional free parameters, a variable surface layer height and the scaling height in the troposphere. Even at only 6 different elevation angles the fit of 4 free parameters was found to be meaningful for most conditions. This was shown by the good correlation with locally measured aerosol extinction, and the deduction of reasonable boundary layer heights between 500 m and 2 km.

The conditions at the Guangzhou backgarden supersite were mainly characterized by strong particulate pollution at ground level. The approach taken here assumed a constant single scattering albedo and asymmetry factor for the entire troposphere. This might not be adequate, even under the conditions of high turbulence and mixing driven by an extremely high solar radiation. In addition, in some cases we had difficulties to constrain the total optical depth. These issues can be addressed by improving the lookup table setup and fitting strategy, however, requiring much more time for the RTM modelling and evaluation of sensitivities. For further experiments, we conclude that measured radiances can improve the evaluation process, as suggested by Friess et al. (2006). Furthermore, additional elevation and azimuth angles or the O_4 absorption at additional wavelengths can be measured and modelled to advance the quality of the aerosol profile retrieval from MAX-DOAS measurements.

Acknowledgements. The authors like to thank R. Sinreich, U. Friess, and U. Platt (Heidelberg) for the lending of the Mini-MAX DOAS instrument, the MiniMax software, and fruitful discussions. The technical help and support at the field site from the PRiDe-PRD2006 campaign team, especially R. Häseler (Jülich), M. Hu, L. Zeng, and Y. Zhang (Beijing) are gratefully acknowledged. We thank all participants of the distributed computing of the RTM. This work was supported by the China National Basic Research and Development Program 2002CB410801, and the National High Technology Research and Development Program of China (863 Program) 2006AA06A301.

References

Arnott, W. P., Moosmuller, H., Rogers, C. F., Jin, T. F., and Bruch, R.: Photoacoustic spectrometer for measuring light absorption by aerosol: instrument description, Atmos. Environ., 33, 2845–2852, doi:10.1016/S1352-2310(98)00361-6, 1999. 17669

Bussemer, M.: Der Ring-Effekt: Ursachen und Einfluss auf die spektroskopische Messung stratosphäischer Spurenstoffe, Master's thesis, Universität Heidelberg, Germany, 1993. 17667

Chiang, C.-W., Chen, W.-N., Liang, W.-A., Das, S. K., and Nee, J.-B.: Optical properties of tropospheric aerosols based on measurements of lidar, sun-photometer, and visibility at Chung-Li (25N, 121E), Atmos. Environ., 41, 4128–4137, doi:10.1016/j.atmosenv.2007.01.019, 2007. 17670

Eck, T., Holben, B. N., Reid, J. S., Dubovik, O., Smirnov, A., O'Neill, N., Slutsker, I., and Kinne, S.: Wavelength dependence of the optical depth of biomass burning, urban, and desert dust aerosols, J. Geophys. Res., 104, 31 333–31 349, 1999. 17673

Friess, U., Monks, P. S., Remedios, J. J., Rozanov, A., Sinreich, R., Wagner, T., and Platt, U.: MAX-DOAS O4 measurements: A new technique to derive information on atmospheric aerosols: 2. Modeling studies, J. Geophys. Res.-Atmos., 111, D14 203, doi:10.1029/2005JD006618, 2006. 17662, 17676

Garland, R. M., Yang, H., Schmid, O., Rose, D., Nowak, A., Achtert, P., Wiedensohler, A., Takegawa, N., Kita, K., Miyazaki, Y., Kondo, Y., Hu, M., Shao, M., Zeng, L., Zhang, Y., Andreae, M. O., and Pöschl, U.: Aerosol optical properties in a rural environment near the mega-city Guangzhou, China: implications for regional air pollution, radiative forcing and

remote sensing, Atmos. Chem. Phys., 8, 5161–5186, 2008, http://www.atmos-chem-phys.net/8/5161/2008/. 17668
Grainger, J. F. and Ring, J.: Anomalous Fraunhofer Line Profiles, J. Geophys. Res.-Atmos., 193, 762, http://dx.doi.org/10.1038/193762a0, 1962. 17667
Greenblatt, G. D., Orlando, J. J., Burkholder, J. B., and Ravishankara, A. R.: Absorption-Measurements of Oxygen between 330nm and 1140nm, J. Geophys. Res.-Atmos., 95, 18 577–18 582, 1990. 17668
Hendrick, F., Van Roozendael, M., Kylling, A., Petritoli, A., Rozanov, A., Sanghavi, S., Schofield, R., von Friedeburg, C., Wagner, T., Wittrock, F., Fonteyn, D., and De Mazire, M.: Intercomparison exercise between different radiative transfer models used for the interpretation of ground-based zenith-sky and multi-axis DOAS observations, Atmos. Chem. Phys., 6, 93–108, 2006, http://www.atmos-chem-phys.net/6/93/2006/. 17665
Hönninger, G. and Platt, U.: Observations of BrO and its vertical distribution during surface ozone depletion at Alert, Atmos. Environ., 36, 2481–2489, doi:10.1016/S1352-2310(02)00104-8, 2002. 17662
Hönninger, G., von Friedeburg, C., and Platt, U.: Multi axis differential optical absorption spectroscopy (MAX-DOAS), Atmos. Chem. Phys., 4, 231–254, 2004, http://www.atmos-chem-phys.net/4/231/2004/. 17662
Inomata, S., Tanimoto, H., Kameyama, S., Tsunogai, U., Irie, H., Kanaya, Y., and Wang, Z.: Technical Note: Determination of formaldehyde mixing ratios in air with PTR-MS: laboratory experiments and field measurements, Atmos. Chem. Phys., 8, 273–284, 2008, http://www.atmos-chem-phys.net/8/273/2008/. 17662
Irie, H., Kanaya, Y., Akimoto, H., Iwabuchi, H., Shimizu, A., and Aoki, K.: First retrieval of tropospheric aerosol profiles using MAX-DOAS and comparison with lidar and sky radiometer measurements, Atmos. Chem. Phys., 8, 341–350, 2008, http://www.atmos-chem-phys.net/8/341/2008/. 17663, 17669
Kraus, S. and Geyer, A.: DOASIS Jscript programming description, Institut für Umweltphysik, Universität, Heidelberg, 2001. 17667
Kurucz, R. L., Furenlid, I. J., and Testerman, L.: Solar Flux Atlas from 296 to 1300 nm, Technical report, National Solar Observatory, 1984. 17668
Leigh, R. J., Corlett, G. K., Frie, U., and Monks, P. S.: Spatially resolved measurements of nitrogen dioxide in an urban environment using concurrent multi-axis differential optical ab-

sorption spectroscopy, Atmos. Chem. Phys., 7, 4751–4762, 2007, http://www.atmos-chem-phys.net/7/4751/2007/. 17662

Meller, R. and Moortgat, G. K.: Temperature dependence of the absorption cross sections of formaldehyde between 223 and 323 K in the wavelength range 225–375 nm, J. Geophys. Res.-Atmos., 105, 7089–7101, 2000. 17667

Perliski, L. M. and Solomon, S.: On the Evaluation of Air-Mass Factors for Atmospheric near-Ultraviolet and Visible Absorption-Spectroscopy, J. Geophys. Res., 98, 10 363–10 374, 1993. 17663

Pikelnaya, O., Hurlock, S. C., Trick, S., and Stutz, J.: Intercomparison of multiaxis and long-path differential optical absorption spectroscopy measurements in the marine boundary layer, J. Geophys. Res., 112, D10S01, doi:10.1029/2006JD007727, 2007. 17662, 17663

Platt, U. and Stutz, J.: Differential Optical Absorption Spectroscopy: Principles and Applications, Springer, Berlin, Heidelberg, Germany, 2008. 17662

Platt, U., Marquard, L., Wagner, T., and Perner, D.: Corrections for zenith scattered light DOAS, Geophys. Res. Lett., 24, 1759–1762, 1997. 17668

Sasano, Y.: Tropospheric aerosol extinction coefficient profiles derived from scanning lidar measurements over Tsukuba, Japan, from 1990 to 1993, Applied Optics, 35, 4941–4952, 1996. 17670

Sinreich, R., Volkamer, R., Filsinger, F., Friess, U., Kern, C., Platt, U., Sebastin, O., and Wagner, T.: MAX-DOAS detection of glyoxal during ICARTT 2004, Atmos. Chem. Phys., 7, 1293–1303, 2007, http://www.atmos-chem-phys.net/7/1293/2007/. 17662

Voigt, S., Orphal, J., Bogumil, K., and Burrows, J. P.: The temperature dependence (203-293 K) of the absorption cross sections of O-3 in the 230-850 nm region measured by Fourier-transform spectroscopy, J. Photoch. Photobio. A, 143, 1–9, 2001. 17667

Voigt, S., Orphal, J., and Burrows, J. P.: The temperature and pressure dependence of the absorption cross-sections of NO2 in the 250-800 nm region measured by Fourier-transform spectroscopy, J. Photoch. Photobio. A, 149, 1–7, 2002. 17667

Wagner, T., Dix, B., von Friedeburg, C., Friess, U., Sanghavi, S., Sinreich, R., and Platt, U.: MAX-DOAS O4 measurements: A new technique to derive information on atmospheric aerosols - Principles and information content, J. Geophys. Res., 109, D22 205, doi:10.1029/2004JD004904, 2004. 17662, 17665, 17666, 17672

Wagner, T., Burrows, J. P., Deutschmann, T., Dix, B., von Friedeburg, C., Frie, U., Hendrick, F., Heue, K.-P., Irie, H., Iwabuchi, H., Kanaya, Y., Keller, J., McLinden, C. A., Oetjen, H., Palazzi, E., Petritoli, A., Platt, U., Postylyakov, O., Pukite, J., Richter, A., van Roozendael, M., Rozanov, A., Rozanov, V., Sinreich, R., Sanghavi, S., and Wittrock, F.: Comparison of box-air-mass-factors and radiances for Multiple-Axis Differential Optical Absorption Spectroscopy (MAX-DOAS) geometries calculated from different UV/visible radiative transfer models, Atmos. Chem. Phys., 7, 1809–1833, 2007, http://www.atmos-chem-phys.net/7/1809/2007/. 17665

Wilmouth, D. M., Hanisco, T. F., Donahue, N. M., and Anderson, J. G.: Fourier transform ultraviolet spectroscopy of the A(2)Pi(3/2) ¡- X(2)Pi(3/2) transition of BrO, J. Phys. Chem. A, 103, 8935–8945, 1999. 17667

Wittrock, F., Oetjen, H., Richter, A., Fietkau, S., Medeke, T., Rozanov, A., and Burrows, J. P.: MAX-DOAS measurements of atmospheric trace gases in Ny-Ålesund - Radiative transfer studies and their application, Atmos. Chem. Phys., 4, 955–966, 2004, http://www.atmos-chem-phys.net/4/955/2004/. 17662

Table 1. Parameters for Lookup table (LUT) generation. SZA: solar zenith angle. SRAA: solar relative azimuth angle. F: fraction of the total extinction residing in the boundary layer. SSA: single scattering albedo. g: asymmetry parameter. τ: aerosol optical depth (see Eq. 6). H: height of the boundary layer. ξ: scaling height of aerosol extinction in the free troposphere. #: number of McArtim runs for the setup of the LUT.

		parameter for both, A4 and A5	
SZA	[deg]	80.92, 69.58, 55.88, 42.19, 28.65, 14.72, 4.02, 13.22, 26.86, 40.75, 54.29, 67.66, 80.05	
SRAA	[deg]	−19.72, −15.43, −11.09, −7.12, −2.82, 3.25, 80.82, 175.33, 182.36, 186.63, 190.64, 194.67, 199.13	
F		0.1–1.0 (interval: 0.1)	
SSA		0.85	
g		0.68	
		A4	A5
τ	[km^{-1}]	0.05, 0.15, 0.30, 0.45, 0.60, 1.0, 1.5, 2.0, 3.0	0.05, 0.15, 0.3, 0.6, 1.0, 1.5, 2.0, 2.5, 3.0, 3.5, 4.0, 4.5
H	[km]	0.4	0.1, 0.3, 0.5, 0.7, 1.0, 1.5
ξ	[km]	3.0	1.0, 3.0, 5.0, 7.0, 9.0
#		10648	46800

ACPD
8, 17661–17690, 2008

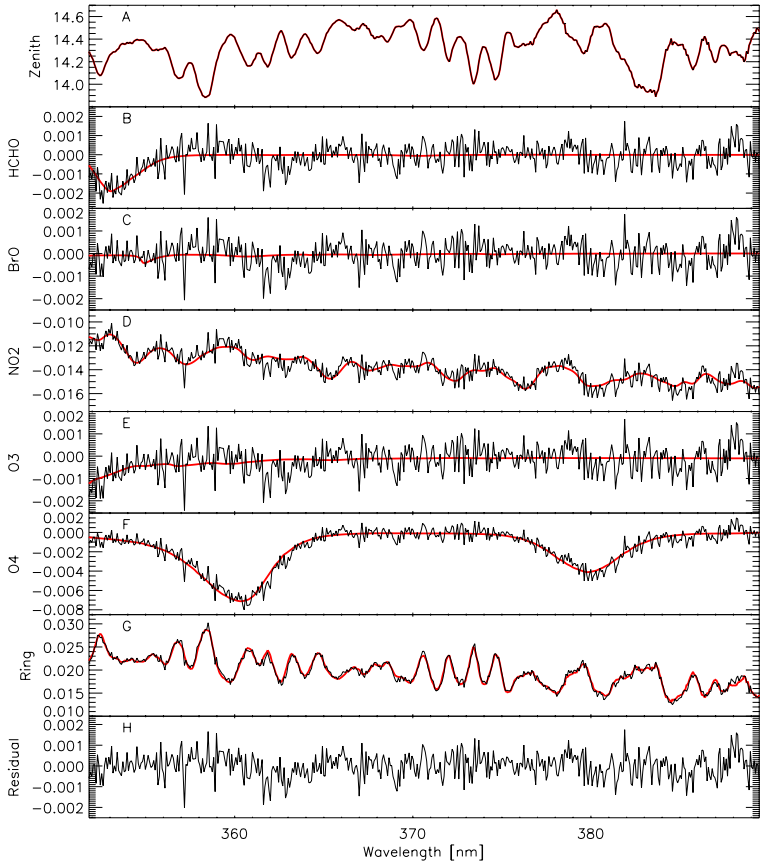

Fig. 1. Evaluation of a single spectrum (α=3°) recorded in the wavelength range 352 nm to 390 nm used for the O_4 determination on 19 July 2006 at 10:59. **(a)** overlay of spectrum at 3° with fitted zenith spectrum. **(b)**, **(c)**, **(d)**, **(e)**, **(f)** fitted HCHO, BrO, NO_2, O_3, and O_4 reference spectrum overlayed to the residual including the absorption.

ACPD
8, 17661–17690, 2008

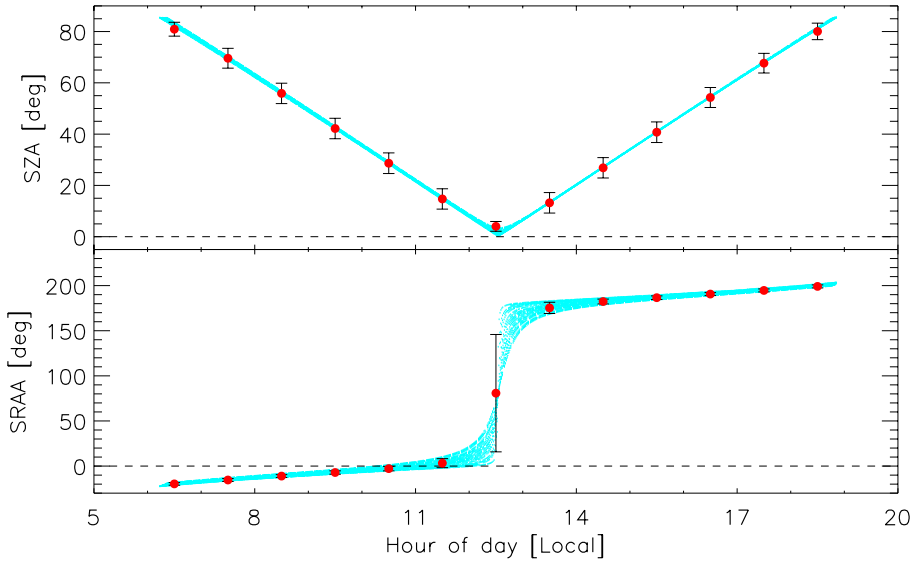

Fig. 2. Range of solar zenith angles and azimuth angles during the entire campaign. The blue symbols refer to the values of each single recorded spectrum, the red refer to the values used in the RTM calculation (see Table 1).

ACPD
8, 17661–17690, 2008

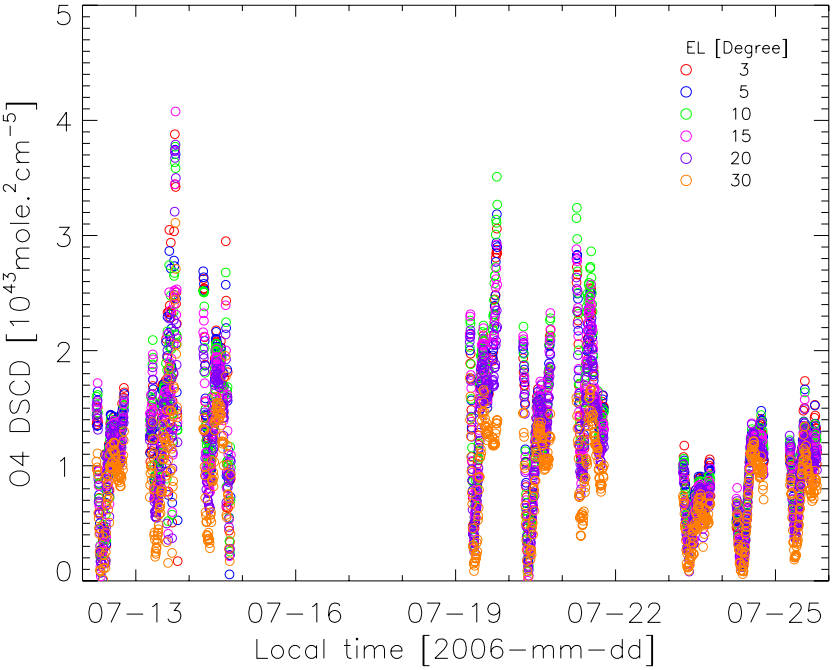

Fig. 3. Differential slant column densities of O_4 measured on cloud free days during the PRiDe PRD2006 campaign. Low values on 23–25 Jul 2006 refer to high aerosol loads close to the surface.

ACPD
8, 17661–17690, 2008

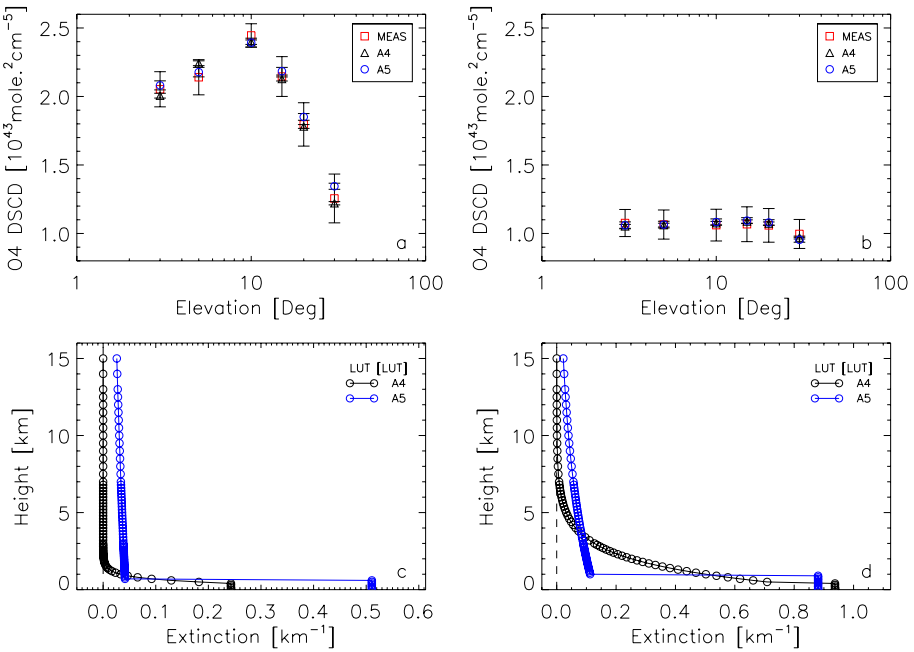

Fig. 4. Two examples for the retrieval of the aerosol profiles with different aerosol loads. Upper row: comparison of measured and modelled O_4 DSCDs. Lower row: retrieved profiles for the A4 and A5 LUTs. Left: 21 July 2006, 11:00–12:00, SZA=15°. Right: 24 July 2006, 12:00–13:00, SZA=15°.

ACPD
8, 17661–17690, 2008

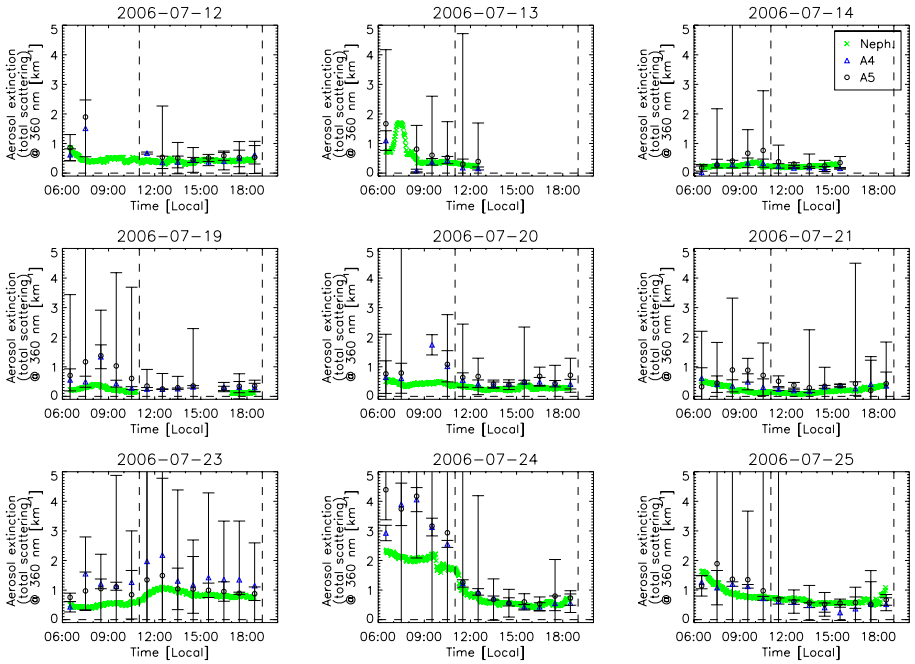

Fig. 5. Hourly mean data of aerosol extinction in the lowest layer derived from the MAX-DOAS (blue triangle and black circle) compared to nephelometer measurements.

ACPD
8, 17661–17690, 2008

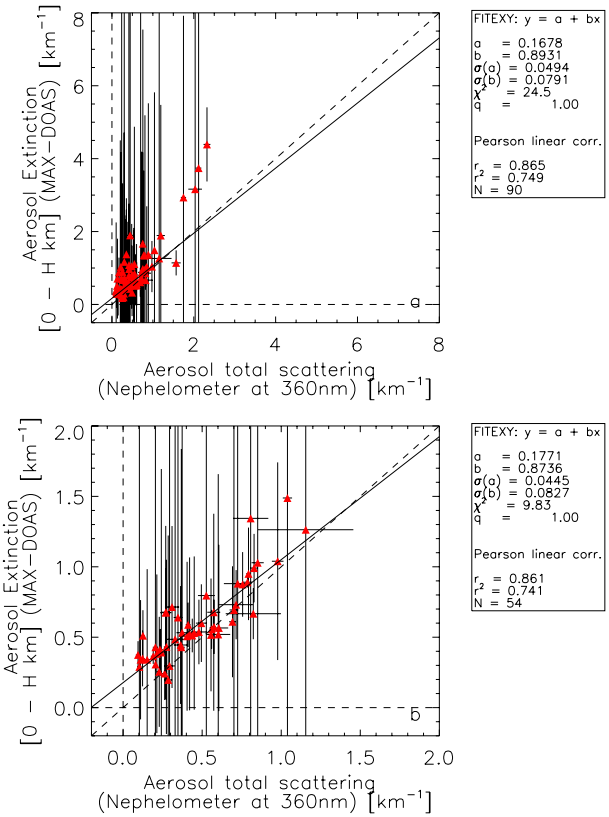

Fig. 6. Regression and correlation analysis of MAX-DOAS aerosol versus nephelometer data. Upper figure: all data recorded during 9 days.

ACPD
8, 17661–17690, 2008

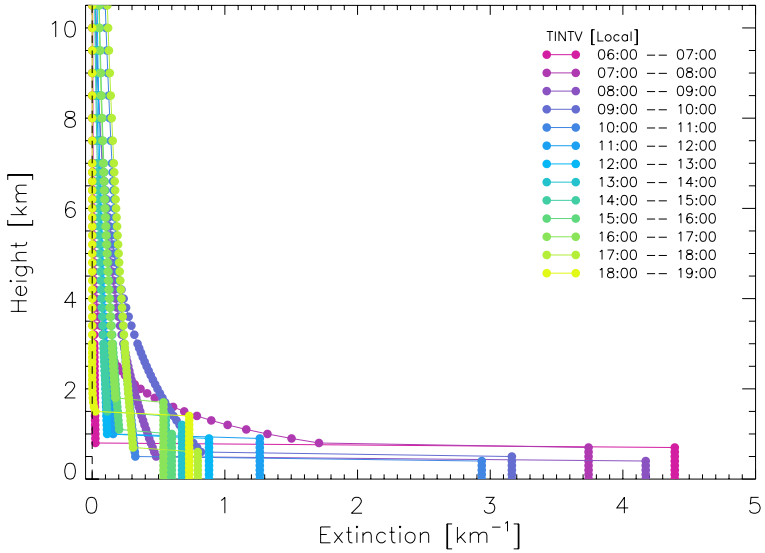

Fig. 7. Evolution of the hourly mean aerosol vertical profile on 24 July 2006 as derived from A5 run.

ACPD
8, 17661–17690, 2008

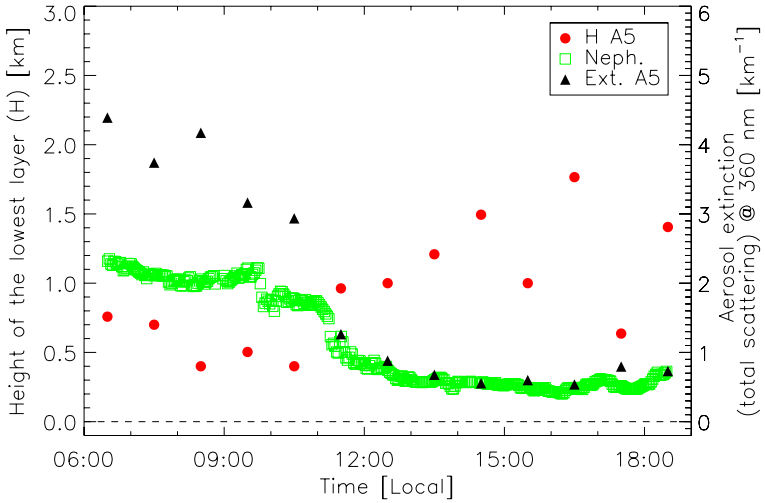

Fig. 8. Results of the aerosol extinction in the lowest layer (black triangle) and the height of this layer (red dot) on 24 July 2006 derived from A5 run. Aerosol total scattering at 360 nm derived from nephelometer measurement (green square).

ACPD
8, 17661–17690, 2008

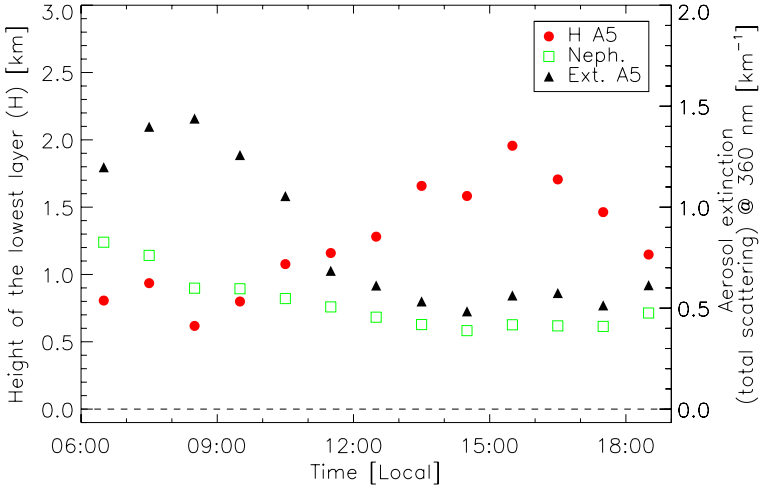

Fig. 9. Average diurnal profiles (based on 9 days, see Fig. 5). The boundary layer height *H* and the aerosol extinction were deduced from the A5 run. The nephelometer data are averaged over 1-h intervals.

ACPD
8, 17661–17690, 2008